

## Muon diffusion in intermetallic compounds of the MoSi<sub>2</sub>-type structure

This article has been downloaded from IOPscience. Please scroll down to see the full text article.

2001 J. Phys.: Condens. Matter 13 5285

(<http://iopscience.iop.org/0953-8984/13/22/321>)

View [the table of contents for this issue](#), or go to the [journal homepage](#) for more

Download details:

IP Address: 171.66.16.226

The article was downloaded on 16/05/2010 at 13:26

Please note that [terms and conditions apply](#).

# Muon diffusion in intermetallic compounds of the MoSi<sub>2</sub>-type structure

P J Mendes, L P Ferreira, J M Gil and N Ayres de Campos

Physics Department, University of Coimbra, P-3004-516 Coimbra, Portugal

Received 28 November 2000, in final form 28 March 2001

## Abstract

The localization and diffusion of positive muons are studied in three binary metallic systems, Zr<sub>2</sub>Cu, Hf<sub>2</sub>Cu and Ti<sub>2</sub>Cu, presenting the MoSi<sub>2</sub>-type structure. Zero-field  $\mu$ SR measurements are interpreted as the muons being static in the T<sub>b</sub>/O<sub>b</sub> interstitial site at low temperatures and, as the temperature is increased, starting diffusing through the network of T<sub>b</sub> sites around the O<sub>b</sub> site, until they reach a state occupying simultaneously the four T<sub>b</sub> sites. Long-range diffusion is observed above 300 K. Activation energies for the lower-temperature diffusion processes are obtained. The results are interpreted in terms of the lattice structure characteristics.

## 1. Introduction

Detailed information on the static and dynamic properties of muons, as interstitial particles in materials, can be obtained by  $\mu^+$ SR spectroscopy [1]. Muons are sensitive to the magnitude, symmetry and fluctuations of local surrounding magnetic fields, yielding information on the environment where they are located. Positive muons are in many aspects similar to protons and therefore valuable information on the static behaviour of hydrogen in materials can be deduced by this method. Muon diffusion parameters, although not immediately transferable to the hydrogen case, provide information useful for the study of hydrogen diffusion processes [2, 3].

This work is part of a study of positive muon diffusion and localization in binary alloys embracing the study of its crystal structure dependence for the same elemental composition and its dependence on the elemental composition for the same structure. The work presented in this paper consists of the study by  $\mu^+$ SR spectroscopy of the behaviour of implanted muons in a series of binary alloys presenting the same MoSi<sub>2</sub> crystallographic structure. The alloys under study were Zr<sub>2</sub>Cu, Hf<sub>2</sub>Cu and Ti<sub>2</sub>Cu. They crystallize in the tetragonal MoSi<sub>2</sub>-type structure belonging to the *I4/mmm* space group. Cu occupies the 2a (0, 0, 0) position and Zr (Hf or Ti) occupies the 4e (0, 0, z) position as shown in figure 1.

## 2. Experimental details and results

Polycrystalline samples were prepared from high purity elements by HF melting under an argon atmosphere. X-ray diffraction using a high resolution transmission diffractometer was

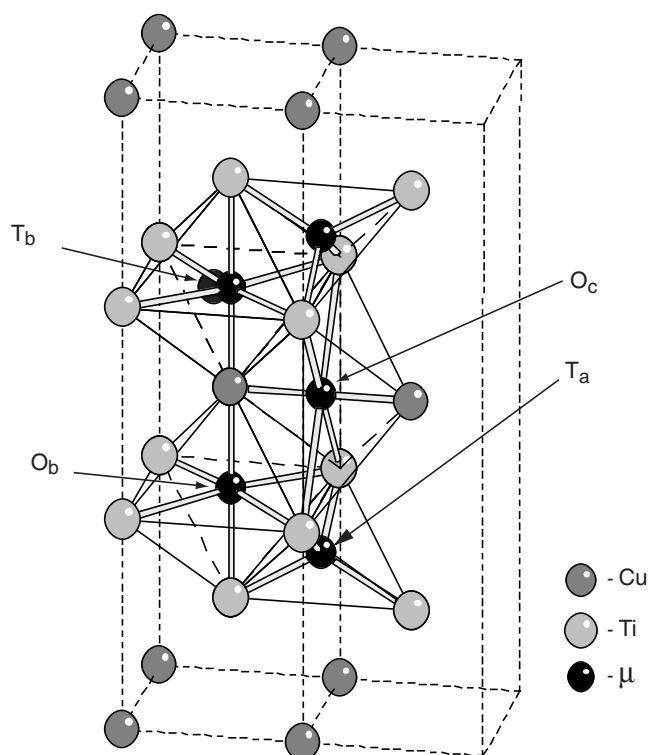


**Figure 1.** Tetragonal unit cell of the MoSi<sub>2</sub>-type structure, showing some of the interstitial sites available for the muon. There are four T<sub>b</sub> sites surrounding each O<sub>b</sub> site.

**Table 1.** Lattice parameters, *z* coordinate and unit cell volume for Zr<sub>2</sub>Cu, Hf<sub>2</sub>Cu and Ti<sub>2</sub>Cu.

Sample	<i>a</i> (Å)	<i>c</i> (Å)	<i>z</i> (Å)	Unit cell volume (Å <sup>3</sup> )
Zr <sub>2</sub> Cu	3.218 (1)	11.186 (1)	0.3456 (1)	115.9
Hf <sub>2</sub> Cu	3.168 (1)	11.137 (1)	0.3449 (2)	111.8
Ti <sub>2</sub> Cu	2.935 (2)	10.772 (2)	0.3320 (9)	92.8

used to verify the crystallographic structures. In all samples we obtained virtually 100% of the desired tetragonal phase. (A typical x-ray spectrum, obtained for Zr<sub>2</sub>Cu, is shown in figure 2.) The lattice parameters and the parameter *z* for the 4e position were obtained for all the samples. The refinement used the Rietveld method and the Fullprof program [4]. The results are presented in table 1.

$\mu^+$ SR measurements were carried out in zero applied field and longitudinal geometry using the ISIS pulsed muon source at the Rutherford Appleton Laboratory, UK (EMU and MuSR lines). The alloys were reduced to powder and circular samples with 20 mm diameter and 1 mm thickness were prepared. Measurements were carried out in a temperature range from 15 K to 330 K. The background signal, originated from muons stopped in the sample environment, was determined using an ErAl<sub>2</sub> sample in a transverse-field measurement at 20 G [5]. Typical zero-field  $\mu^+$ SR spectra at different temperatures for Zr<sub>2</sub>Cu are illustrated in figure 3.

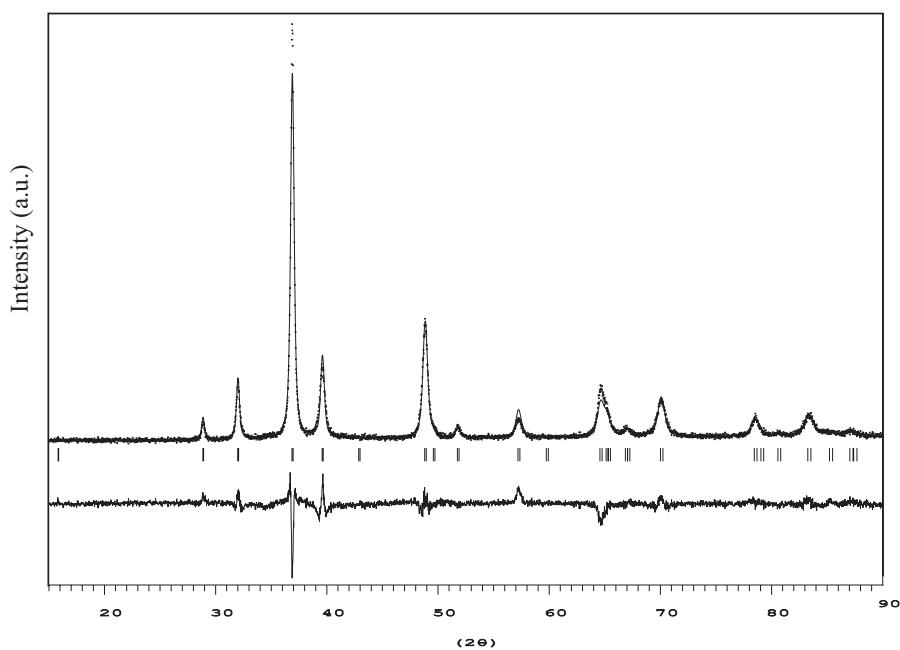


**Figure 2.** Experimental (dots) and calculated (lines) x-ray diffraction patterns for  $Zr_2Cu$ . The difference pattern (observed – calculated) is shown at the bottom of the figure.

### 3. Analysis and discussion

#### 3.1. Preliminary analysis

A series of fits to the experimental data using a single static Kubo–Toyabe (K–T) function [6, 7]

$$P_z(t) = \frac{1}{3} + \frac{2}{3}(1 - \Delta^2 t^2) \exp(-\frac{1}{2} \Delta^2 t^2) \quad (1)$$

was first considered. In this equation,  $z$  is the direction of the initial muon spin polarization, coincident with the beam direction in the longitudinal geometry set-up, and  $\Delta$  is the width of the isotropic Gaussian distribution of the local magnetic fields, which are considered to be static and random. The  $1/3$  term corresponds to the fraction of muons that are at positions where the local field is aligned either parallel or antiparallel to the initial spin polarization, while the remaining  $2/3$  of the spin polarization precesses due to the transverse local field components.

The  $\Delta$  values obtained from the fits are presented in figure 4 as a function of temperature. For all compounds, three distinct regions can be identified: one, at low temperatures, showing a plateau in the value of  $\Delta$ ; another, where  $\Delta$  decreases with increasing temperature; and a third region, where  $\Delta$  seems to attain a new plateau with a lower  $\Delta$ . In  $Zr_2Cu$ , a new decrease of  $\Delta$  can be guessed from the value at the highest temperature. The average values of  $\Delta$  in the first ( $\Delta_1$ ) and the third ( $\Delta_2$ ) region of temperature plateaus are presented in the first columns of table 2.

A first possible interpretation is as follows. The muon is static at low temperatures, the  $\Delta_1$  values characterizing the local nuclear fields experienced by the muon in the occupied sites. The decrease of  $\Delta$  observed in the second region corresponds to motional narrowing, indicating muon diffusion. If long-range diffusion takes place, it is expected that the muon

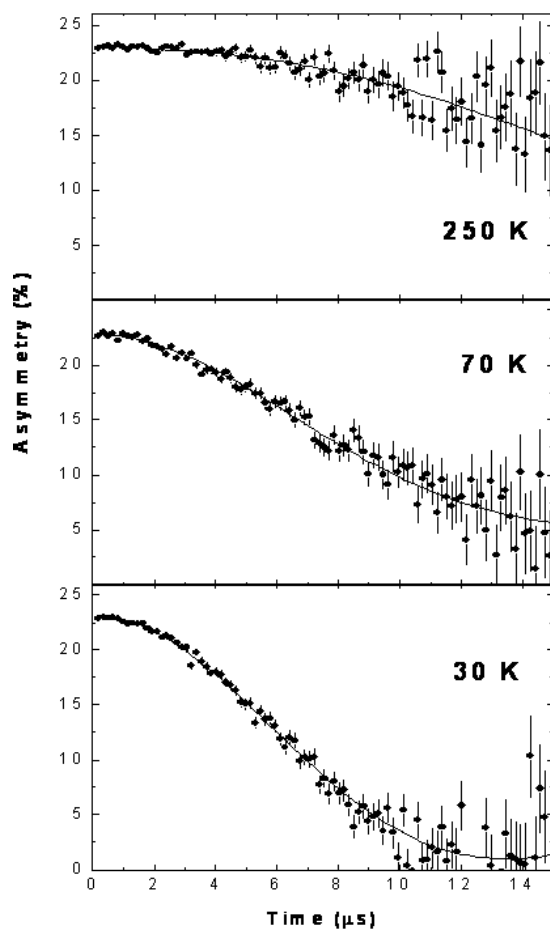


**Figure 3.**  $\mu^+$  decay asymmetry obtained for  $\text{Zr}_2\text{Cu}$  in zero applied field, at different temperatures. The solid lines are fits using the function in equation (2).

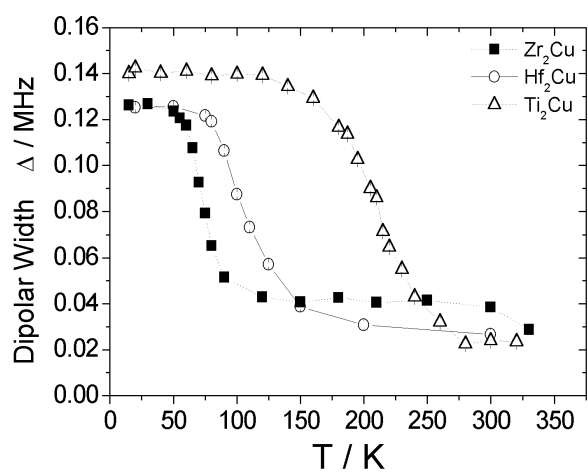


**Figure 4.** Width  $\Delta$  of the local field distribution as a function of temperature for the three samples. The lines are only guides to the eye.

**Table 2.** Width of the distribution (MHz) of the static dipolar fields in the Van Vleck limit, calculated at different interstitial positions available for the muon in the MoSi<sub>2</sub>-type structure. Extracted from figure 4 and shown for comparison are:  $\Delta_1$ —plateau values of  $\Delta$  (MHz) at low temperatures for the three samples;  $\Delta_2$ —plateau values of  $\Delta$  (MHz) at high temperatures. In the first row, the numbers in parenthesis correspond to the number of interstitial sites by formula unit.

Sample	$\Delta_1$	$\Delta_2$	(2) O <sub>a</sub>	(4) O <sub>b</sub>	(4) O <sub>c</sub>	(4) T <sub>a</sub>	(16) T <sub>b</sub>	(8) T <sub>c</sub>
Zr <sub>2</sub> Cu	0.127(1)	0.041(2)	0.139	0.152	0.276	0.056	0.148	0.191
Hf <sub>2</sub> Cu	0.125(1)	0.027(2)	0.145	0.147	0.290	0.058	0.148	0.198
Ti <sub>2</sub> Cu	0.140(1)	0.023(2)	0.183	0.172	0.364	0.068	0.166	0.261

does not stop in any specific site and so the motional narrowing should continue until a zero mean value is reached. The observation of a plateau in the third temperature region can be interpreted as the muons being stopped at a different site, characterized by the  $\Delta_2$  values. A second diffusion process from the latter sites would explain the decrease in  $\Delta$  above 300 K for Zr<sub>2</sub>Cu.

### 3.2. Muon sites in the MoSi<sub>2</sub> structure

Assuming that the muons are static at the high and low temperature plateaus an identification of the occupied sites was tried by a careful study of the interstitial sites available for the muon in the lattice followed by calculations of the corresponding depolarization rates expected in the Van Vleck limit.

In figure 1, some of the interstitial sites available for muon occupation in the MoSi<sub>2</sub> type structure are shown. Due to their large size and strong electronic affinity for hydrogen isotopes, three octahedral sites—O<sub>a</sub>, O<sub>b</sub> and O<sub>c</sub>, coordinated, respectively, by (4 Cu, 2 Zr), (1 Cu, 5 Zr) and (2 Cu, 4 Zr)—and three tetrahedral sites—T<sub>a</sub>, T<sub>b</sub> and T<sub>c</sub>, coordinated, respectively, by (4 Zr), (1 Cu, 3 Zr) and (2 Cu, 2 Zr) were considered.

Using the Van Vleck approximation for non-identical spins [8], it is possible to calculate the second moment of the local magnetic field distribution created by the surrounding nuclear magnetic moments at each interstitial site. The zero-field dipolar width  $\Delta$  is directly derived from this second moment. Calculations were carried out using the positions of the Zr (Hf or Ti) and Cu atoms found on the x-ray analysis and introducing nuclear magnetic moments on the Cu atoms alone. This is justified by the fact that all Cu nuclei are magnetic (69% of <sup>63</sup>Cu have a nuclear moment of 2.22  $\mu_N$  and 31% of <sup>65</sup>Cu have a nuclear moment of 2.38  $\mu_N$ ) [9]. On the other hand, most natural titanium, hafnium and zirconium nuclei are non-magnetic and those isotopes having a magnetic moment different from zero have very low abundances. The natural abundance of <sup>91</sup>Zr, that has the highest moment (−1.3  $\mu_N$ ), is only 11%. It was calculated that even a contribution of 100% for this isotope would increase the  $\Delta$  values by only less than 10%. The contribution of these nuclei was therefore neglected in our calculations.

Although the local lattice expansion due to the polaron effect seems difficult to evaluate, published results comparing theoretical and experimental  $\Delta$  values [3, 10], have led us to consider a reduction of 20% on the calculated values of  $\Delta$ . The results are shown in table 2.

### 3.3. Muon localization

Comparing the experimental  $\Delta_1$  values at low temperatures with the calculated values (table 2) a statistical distribution of the muons among the different interstitial sites [11] did not seem appropriate since the weighted average of the dipolar width of the available interstitial sites is 20% to 40% larger than the experimental values. According to the values presented in table 2

the most probable sites for muon occupancy are interstitials  $O_b$  and  $T_b$ .  $O_a$  sites present also a convenient  $\Delta$  value in the case of  $Zr_2Cu$  and  $Hf_2Cu$  but its size is more than 50% smaller. Tetrahedral sites  $T_b$ , with three Zr (Hf or Ti) atoms as coordination, are the largest sites in the unit cell, and form closed and large paths around  $O_b$ . Good fits to the data are obtained at these low temperatures using a static Kubo–Toyabe function. We assume that the  $\Delta$  plateaus correspond to muons static at the  $O_b$  or  $T_b$  sites. A potential reason for the difference between theoretical and experimental values of  $\Delta$  is either a polaron effect more important than 20% or a higher order influence of additional interactions. One possibility would be the quadrupole interaction due to the electric field gradient produced by the muonic charge [12]. However, as in recent transverse field measurements in a different binary intermetallic compound,  $Ti_2Co$ , with fields up to 0.6 T no change of the dipolar linewidth could be detected, this possibility might not be appropriate.

To assign an interstitial site to the high temperature plateau with  $\Delta_2$  values, as presented in table 2, it is apparent that the closest calculated values are for the  $T_a$  site. Other interstitial positions, mainly or totally coordinated by Zr (Hf or Ti) atoms have a rather small size and the corresponding values of  $\Delta$  are larger than the values found for sites  $T_a$ , and were therefore discarded. The site with the smallest calculated  $\Delta$  is a substitutional position of Cu, a site with eight Zr atoms in the first neighbourhood. The  $\Delta$  calculated for this position (including the polaron effect) was 0.054 MHz for  $Zr_2Cu$ , 0.057 MHz for  $Hf_2Cu$  and 0.071 MHz for  $Ti_2Cu$ . These values are very similar to those calculated for the interstitial site  $T_a$ . A discrepancy is found when noticing that the calculated  $\Delta$  values increase for all considered sites from Zr to Ti, while the experimental  $\Delta_2$  values decrease.

This discrepancy indicates that the simple static muon interpretation presented for the low temperature case, does not apply in this case and a more complex muon behaviour has to be considered. This is presented below.

### 3.4. Muon diffusion

The above discussions suggest a reanalysis of the data considering the effect of muon motion on the spin depolarization.

The effects of muon diffusion are generally described within the framework of the strong collision model [6, 13]. The muon is assumed to occupy equivalent sites successively, jumping at random times with an average frequency  $\nu_d$ . The time of a jump is taken to be much shorter than the mean residence time at one site. The model also assumes that there is no correlation between the local field experienced by the muon before and after the jump. The total depolarization function within this model (dynamic K–T function) can then be written as

$$G(t) = G(0, t) \exp(-\nu_d t) + \nu_d \int_0^t G(\nu_d, t' - t) \exp(-\nu_d t) G(0, t') dt' \quad (2)$$

where  $\nu_d$  is the correlation frequency (or jump rate) characteristic of the fluctuations of the dipolar interaction between the diffusing muon and the surrounding nuclear magnetic moments, and  $G(0, t)$  is the static depolarization function, in this case assumed to be the static Kubo–Toyabe formula (equation (1)).

The data were reanalysed using formula (2). Assuming that the muon diffuses through the sites characterized by a  $\Delta_1$  value, for each of the compounds the respective value was taken as a fixed parameter in the fitting at all temperatures.

The jump rates obtained are presented in figure 5 as Arrhenius plots. It is observed that for a certain temperature range depending on the compound the muon is involved in an activated diffusion process, the jump rates following an Arrhenius behaviour. This corresponds to the temperature ranges of motional narrowing in figure 4. The onset temperature of the motional

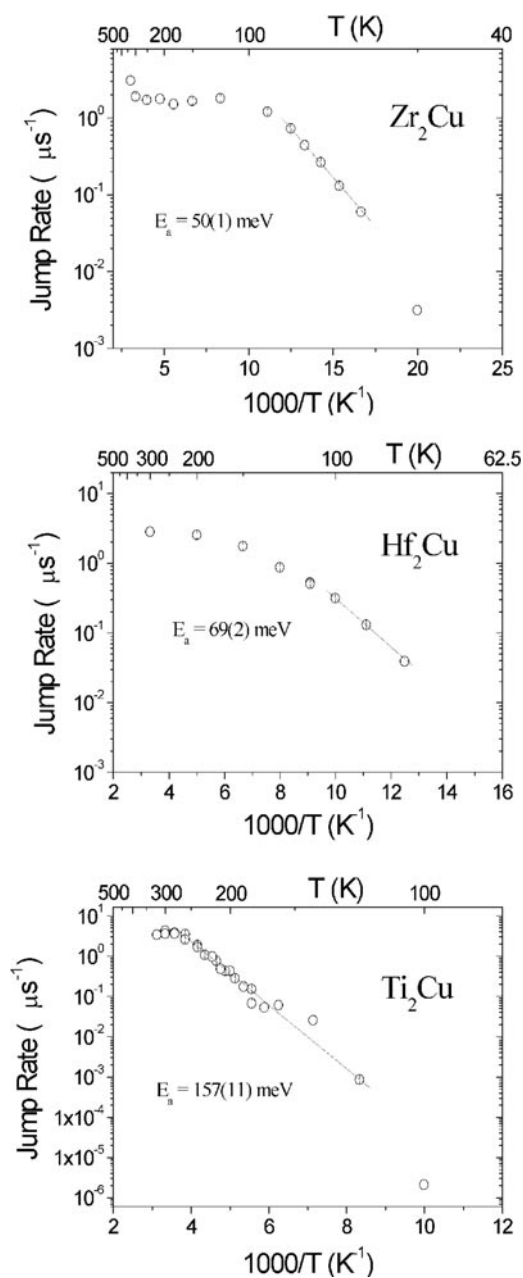


**Figure 5.** Arrhenius plots of the jump rate in  $\text{Zr}_2\text{Cu}$ ,  $\text{Hf}_2\text{Cu}$  and  $\text{Ti}_2\text{Cu}$ . The lines are the results of fits of an exponential function yielding the indicated activation energies  $E_a$ .

narrowing is the lowest for  $\text{Zr}_2\text{Cu}$ , the compound with the highest unit cell volume, and much higher for  $\text{Ti}_2\text{Cu}$  (with the smaller unit cell—see table 1). This means that muons require less energy to move out of the  $T_b/O_b$  sites in the larger unit cells of  $\text{Zr}_2\text{Cu}$  and  $\text{Hf}_2\text{Cu}$ . Activation energies were drawn from fits to the pertaining experimental points in the Arrhenius plots: the values found were 50(1) meV for  $\text{Zr}_2\text{Cu}$ , 69(2) meV for  $\text{Hf}_2\text{Cu}$ , and 157(11) meV for



Ti<sub>2</sub>Cu.

Above a temperature depending on the compound, the fitting procedure with fixed  $\Delta_1$  no longer gives a good description of the data, yielding a constant jump rate value, no longer following an Arrhenius behaviour. We conclude that the activated diffusion process is interrupted.

A trapping and detrapping mechanism due to impurities or structural defects, which would seem to be a plausible interpretation of this behaviour, was discarded for the following reason. The average distance travelled by the muons in these trapping situations (in the present case the muon jump rate being of the order of  $1 \mu\text{s}^{-1}$  at the temperature considered) would imply a high concentration of defects, which is not the case in our samples.

Our interpretation is that the muon is thought to be static at  $T_b$  sites in the lower temperature range. At the onset of motional narrowing, the muon starts to diffuse within a local set of  $T_b$  sites (the four equivalent sites around an  $O_b$  site), in an activated diffusion process. Muons cannot leave the  $O_b$  cage due to the high barrier for jumping into the  $T_a$  sites, which are the next neighbouring sites with the highest probability of occupation due to the proximity (they share faces with  $T_b/O_b$ ) and electronic affinity to the muon. The diffusion through the identical  $T_b$  sites implies a depolarization that should be well fitted with a dynamical K–T function, and that was confirmed. This type of localized motion has already been observed for hydrogen in intermetallic C15-type Laves phases using NMR and QNS [14, 15].

With increasing temperature, the muon acquires enough energy to be insensitive to the potential barriers within the cage, its wavefunction occupying the four  $T_b$  sites and the  $O_b$  site as well. The depolarization function is then equivalent to that of a static muon with a  $\Delta$  value lower than the values calculated for the single sites [16, 17], as was indeed found in the preliminary analysis for the highest temperature plateaus (figure 4).

The mentioned barrier to jump to the  $T_a$  sites would be overcome at higher temperatures, starting a process of long-range diffusion. Such behaviour seems to be perceived in the cases of Zr<sub>2</sub>Cu and Hf<sub>2</sub>Cu. Actually, a small dynamic contribution ( $v_d$ ) was detected at the highest temperature: 330 K for Zr<sub>2</sub>Cu and 300 K for Hf<sub>2</sub>Cu, in fits with a dynamic K–T function with  $\Delta_2$  as dipolar width.

#### 4. Conclusions

The results obtained for muon localization and diffusion in Zr<sub>2</sub>Cu, Hf<sub>2</sub>Cu and Ti<sub>2</sub>Cu suggest that the muon occupies a  $T_b$  or  $O_b$  site at low temperatures.

In the motional narrowing regime, the muon performs a short-range diffusion within the network of  $T_b$  sites. From the Arrhenius behaviour of the jump rate with temperature, the activation energies which characterize this process have been estimated for each compound. From the results and from the temperature at which diffusion sets in, it can be deduced that this activated diffusion process requires less energy in the larger unit cells.

A third regime is observed in these compounds when the jump rate increases to about  $1 \mu\text{s}^{-1}$ . The activated diffusion process is interrupted when the muon has enough energy to occupy simultaneously the four  $T_b$  sites in the  $O_b$  network. This behaviour is similar to a trapping process, but without diffusion to a long distance from the original site. Long-range diffusion is perceived only at temperatures above 300 K.

The  $\mu^+$ SR results presented in this work suggest that structural reasons, in this case the different size of the atoms Zr, Hf and Ti and the consequent differences in the cell volumes, are responsible for the different muon behaviour observed in the three alloys under study.

## Acknowledgments

The authors would like to thank Vitor Amaral (Physics Department, University of Porto) for laboratory facilities in sample preparation, A Matos Beja and J A Paixão (Physics Department, University of Coimbra) for x-ray diffraction facilities and P Dalmas de Réotier (Magnetism and Synchrotron Radiation Laboratory, Centre d'Études Nucléaires de Grenoble) for allowing the use of his computer code for nuclear depolarization rate calculations. This work was supported by PRAXIS XXI (Portugal, PRAXIS/2/2.1/FIS/462/94) and the EU TMR programme for Large Scale Facilities (research at ISIS).

## References

- [1] Cox S F J 1987 *J. Phys. C: Solid State Phys.* **20** 3187
- [2] Hempelmann R, Richter D, Hartmann O and Wäppling R 1990 *Hyperfine Interact.* **64** 649
- [3] Baudry A, Boyer P, Ferreira L P, Harris S W, Miraglia S and Pontonnier L 1992 *J. Phys.: Condens. Matter* **2** 106
- [4] Rodriguez Carvajal J 1990 *Abstracts Satellite Meeting XVth Congress of the IUCr (Toulouse, 1990)* p 127
- [5] Dalmas de Réotier P, Yaouanc A, Eaton G H and Scott C A 1990 *Hyperfine Interact.* **65** 1113
- [6] Hayano R S, Uemura Y J, Imazato J, Nishida N, Yamazaki T and Kubo R 1979 *Phys. Rev. B* **20** 850
- [7] Kubo R and Toyabe T 1966 *Magnetic Resonance and Relaxation* ed R Blinc (Amsterdam: North-Holland) p 810
- [8] Van Vleck J H 1948 *Phys. Rev.* **74** 1168
- [9] Lederer C M, Hollander J M and Perlman I 1967 *Tables of Isotopes* 6th edn (New York: Wiley)
- [10] Karlsson E B 1995 *Solid State Phenomena* (Oxford: Clarendon)
- [11] Hempelmann R, Richter D, Hartmann O, Karlsson E and Wäppling R 1989 *J. Chem. Phys.* **90** 1935
- [12] Hartmann O 1977 *Phys. Rev. Lett.* **39** 832
- [13] Kehr K W, Honig G and Richter D 1978 *Z. Phys. B* **32** 49
- [14] Skripov A V, Soloninin A V, Stepanov A P and Kozhanov V N 1999 *J. Phys.: Condens. Matter* **11** 10393
- [15] Skripov A V, Cooke J C, Udovic T J and Kozhanov V N 2000 *Phys. Rev. B* **62** 14099
- [16] Lankford W F, Birnbaum H K, Fiory A T, Minnich R P, Lynn K G, Stronach C E, Bieman L H, Kossler W J and Lindemuth J 1978 *Hyperfine Interact.* **4** 833
- [17] Sugimoto H and Fukai Y 1980 *Phys. Rev. B* **22** 670